Molecular orientation near the surface of a smectic liquid crystal cell showing V-shaped switching by means of attenuated total internal reflection ellipsometry

Shinya Ikeda, Toyokazu Ogasawara, Michi Nakata, Yoichi Takanishi, Ken Ishikawa, and Hideo Takezoe
Department of Organic and Polymeric Materials, Tokyo Institute of Technology, O-okayama, Meguro-ku, Tokyo 152-8552, Japan
(Received 25 September 2000; revised manuscript received 13 December 2000; published 15 May 2001)

Attenuated total internal reflection ellipsometry was used to probe the molecular orientation and switching near the surface of a smectic liquid crystal cell showing V-shaped switching. We find that the switching occurs collectively near the surface as in the bulk. The molecules form a twisted state, but the twist angle relative to the bulk layer normal is small because of compensating twist of the smectic layer normal. As a result, a rather uniform molecular orientation is produced, resulting in high extinction and a high contrast ratio in the absence of a field.

DOI: 10.1103/PhysRevE.63.061703 PACS number(s): 61.30.Eb, 61.30.Gd, 78.20.Jq

I. INTRODUCTION

Recent developments in the display industry have solved most of the technological problems in realizing ideal liquid crystal displays (LCDs). One of the problems that still remains is switching speed. The demand for fast switching is extremely important for the application of LCs in LCD televisions. Ferroelectric and antiferroelectric LCDs (FLCDs and AFLCDs) may provide solutions to the speed problem. In fact, FLCs and AFLCs with threshold characteristics have been proposed for use in passive matrix displays and studied extensively. However, they are essentially on-off devices, so that displaying gray levels and achievement of full color are difficult. On the other hand, significant advances in the manufacturing of thin film transistors (TFTs) have made TFT technology available at relatively low cost. From this viewpoint, active matrix displays using FLCs and AFLCs on TFT are quite promising. In this display mode, continuous transmittance changes in FLC and AFLC cells are utilized in conjunction with a threshold behavior using TFT. So far, several types of electrooptic switching modes for active FLCDs and AFLCDs have been proposed such as V-shaped switching [1–3], monostable switching [4,5], and deformed helix FLC [6] modes. Among them, V-shaped switching has attracted considerable attention because of extensive discussion on the mechanism for particular molecular orientation and switching [1–3,7–19].

V-shaped switching was first demonstrated by Inui *et al.* [1] in a three-component mixture. This mode is characterized by seven factors: (1) threshold free, (2) domain free, (3) hysteresis free, (4) high contrast ratio, (5) wide viewing angle, (6) high speed, and (7) low applied voltage. The switching mechanism was first interpreted by the existence of a hypothetical tilted smectic phase with molecules randomly oriented on a smectic cone [1–3,7]. The explanation was that the azimuthal randomness of molecules gives a complete extinction between crossed polarizers, one of which is parallel to the smectic layer, and an electric-field induced orientational change to a ferroelectric state occurs according to a two-dimensional Langevin process. However, this explanation is inconsistent with the experimental observations of Park *et al.* [8]. Their experiments included various optical techniques, such as birefringence and second-harmonic generation (SHG) as a function of an electric field *E*, switching current and polarized fourier-transformed infrared (FT-IR) spectroscopy. They also carried out SHG interferometry measurements on which they proposed a model for the molecular orientation in the absence of an electric field as well as its dynamic response to a field. In this model they proposed that projections of the layer normal and molecular director onto the glass substrate are coincident in the absence of a field and that the molecules switch collectively on the half cone under application of an alternating electric field [9].

Polarization charge ρ given by $-\mathrm{div}\,\mathbf{P}$, where $\mathbf{P}$ is the polarization, is considered to play a role in the explanation of how the director is stabilized parallel to the layer normal in a tilted smectic phase [9,10]. The scenario is as follows. Because of a surface polar interaction $\mathbf{P}$ at the surfaces is fixed inward or outward, so that $\mathbf{P}$ is splayed throughout the cell and hence the molecular director is in a twisted state. To minimize the polarization charge effect caused by the splayed polarization, the splayed regions are squeezed out from the center of the cell toward both surfaces, so that extended uniform region emerges at the central part of the cell. Then conflict between the polarization charge effect and distortion energy accumulated at the surfaces takes place. A simple simulation using the 4×4 matrix method suggests that the thickness of splayed orientation must be confined to within 50 nm at both surfaces to obtain the contrast ratio of 150:1 experimentally observed [11,12]. This confinement produces large distortion energy, which would inevitably relax the twisted molecular orientation to a less distorted orientation. Recently Clark *et al.* [13] suggested the extreme case in which perfectly uniform alignment is achieved by charge self-interaction.

The above argument suggests the importance of studies on molecular arrangement and switching in the vicinity of surfaces. This motivated us to perform attenuated total internal reflection (ATIR) measurements. This method enables us to see the dynamic molecular motion near the surfaces. In preliminary experiments, we observed that the molecules switch collectively at surfaces as well as in the bulk [14]. In this study, we perform ATIR experiments as a function of penetration depth and show that rotation of the director is

 ©2001 The American Physical Society

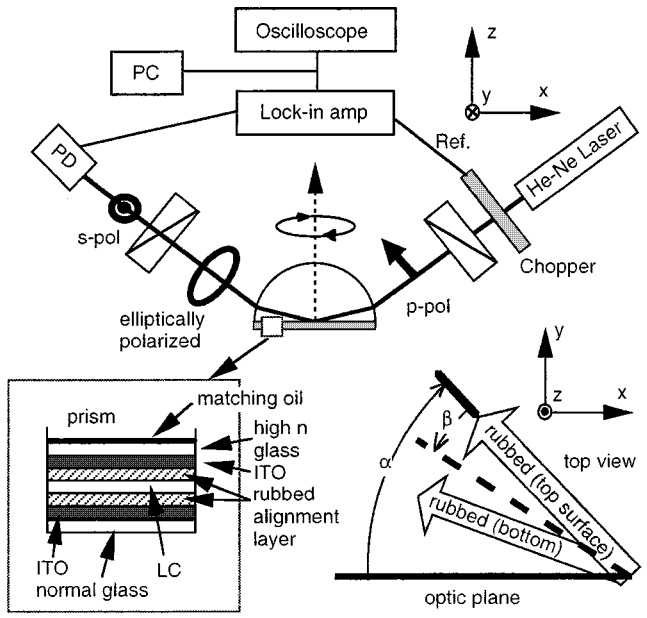

FIG. 1. Optical setup for ATIR measurements. The sample was sandwiched between two (one normal and one high-index) glass substrates, the latter of which was attached to a high-index hemisphere prism with matching oil. Under total internal reflection conditions *p*-polarized light ($\lambda = 633$ nm) was incident on the sample and *s*-polarized reflected light was detected. The measurements were carried out under the application of a triangular wave voltage (0.1 Hz) as a function of cell rotation angle about the surface normal at several incidence angles to vary penetration depth. The cell geometry is also illustrated, where the cell rotation angle α and the angle β specifying the molecular orientation (β_M) or layer normal direction (β_L) are defined as illustrated and as positive for clockwise rotation. In the figure, α is positive and β is negative.

compensated by rotation of the layers to produce a quasiuniform state, leading to a high contrast ratio.

II. EXPERIMENTAL PROCEDURES

The material used in this study is the three-component mixture, that has been extensively used in V-shaped switching experiments [1,2,8–12]. In the smectic X^*(Sm-X^*) phase between 43 and 64 °C below Sm-A, V-shaped switching was observed. The sample was sandwiched between normal and high-index ($n = 1.87852$) glass substrates. The indium tin oxide (ITO) coated glass substrates were spin-coated with polyimide (PI, RN1175, Nissan Chemical) and were rubbed unidirectionally. The thickness and refractive index of ITO were 51.0 nm and 1.860, respectively. Silica beads of 0.97 μm in diameter were used for fabricating cells, giving 1.6–1.8 μm thick cells. Two rubbing directions were crossed by 20 ° (see right bottom in Fig. 1), since the layer normal in the bulk is known to deviate from the rubbing direction because of surface electroclinic effect. As shown in Fig. 1, the high-index glass was attached to high-index hemisphere prism (S-LAH58, Ohara, $n = 1.87852$) with matching oil in-between (Series H-xx, Moritex, $n = 1.891$). The cell was located in an oven, that was designed so that texture observation and electrooptic measurements could be possible.

The optical setup for ATIR measurements is shown in Fig. 1. A *p*-polarized light from a He-Ne laser (5 mW) was focused before entering the hemisphere prism with a lens ($f = 170$ mm) and was collimated by the hemisphere prism, being incident to the cell under a total internal reflection condition. The collimated beam size was about 60 μm in diameter, so that the beam size being incident obliquely at the sample surface was about 120 μm$\times$60 μm. Three goniometers with stepping motors were used to change the incidence angle (Θ scan for the sample stage and 2Θ scan for detection stage with an accuracy of 0.001 °) and to rotate the cell about the cell surface normal (α scan with an accuracy of 0.005°). Careful optical alignment was necessary, particularly since the rotation axis of Θ-2Θ scan is slightly shifted from the prism surface depending on the incidence angle. The polarization direction was also carefully adjusted. The incident light was chopped (480 Hz) and a reflected *s*-polarized light was detected by a diode through a focusing lens ($f = 80$ mm) and was amplified by a lock-in amplifier (EG&G, model 5210).

The total internal reflection takes place for incidence angles larger than 59.1 ° at the interface between ITO and PI, the refractive indices of which are 1.860 and 1.596, respectively. In the evanescent region, light intensity decreases exponentially with distance from the interface. The penetration depth is defined as a length where the light intensity decreases to $1/e$. In the present case, the evanescent region starts from the interface of ITO and PI. On the other hand, the reflection signal originates only from the anisotropic region, since isotropic media cannot change polarization state of the reflected beam. In the present case, the reflection signal is one order of magnitude smaller when the liquid crystal material is in the isotropic phase than that in the liquid crystal phase. This negligibly small signal originates from the anisotropy of rubbed PI. To compensate this small contribution by the PI layer, the signal obtained in the isotropic phase was subtracted from the signal in the liquid crystal phases. In this way the resultant signal originates from the anisotropic liquid crystal layer. Therefore, we define the penetration depth as a length where the light intensity becomes $1/e$ of the intensity at the interface between PI and LC. Since we change the incidence angle between 60° and 68°, the penetration depth varies between 462 and 154 nm. The measurements were made under static and dynamic conditions as a function of cell rotation angle α, that is defined as the angle between the optic plane and the rubbing direction at the top surface being positive for clockwise rotation of the rubbing direction (see right bottom in Fig. 1). For dynamic measurements, *s*-polarized reflected light intensity was detected at a certain angle α under the application of a triangular wave of 0.1 Hz with 24 Vpp. The measurements were repeated after changing α. The signals measured in the isotropic phase at each α were used as a base line to eliminate all the contribution except for the anisotropy of the liquid crystal.

III. SIMULATION

To understand the experimental results, let us first show the simulated results. The simulation was made in the Sm-A

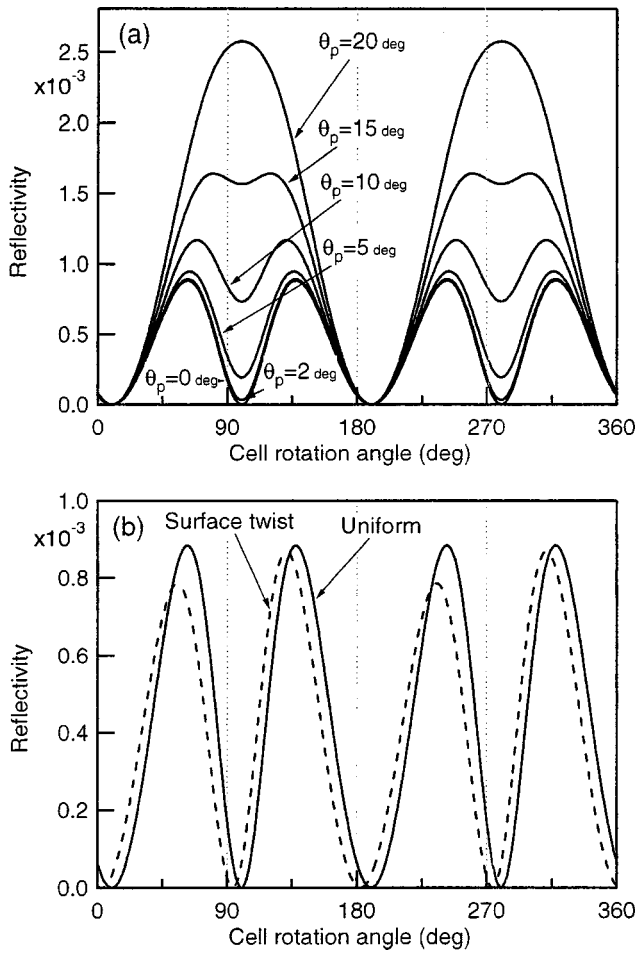

FIG. 2. Simulated reflectivity as a function of cell rotation angle for cells of Sm-*A* (a) with various pretilt angles θ_p and (b) with uniform molecular orientation and with a thin twist region of 20° over 50 nm near the surface.

phase by applying the 4×4 matrix method to the total internal reflection geometry. We neglected the anisotropy of alignment PI layer induced by rubbing and approximated its refractive index to be 1.5 and thickness to be 90 nm. The other parameters used are as follows; the refractive indices of the liquid crystal for ordinary and extraordinary light are, respectively, 1.5 and 1.64, the cell thickness 2 μm and the angle of incidence 68°. To be consistent with the experimental condition, the layer normal in the bulk was assumed to be along the bisector of the rubbing directions at the top and bottom surfaces, i.e., 10° from both.

Figure 2(a) shows *s*-polarized reflected light intensity as a function of cell rotation angle α. The simulation was made for molecular orientations with various pretilt angles $\theta_p = 0°$, 2°, 5°, 10°, 15°, and 20°. If molecules lie parallel to a surface ($\theta_p = 0°$), zero reflectance is obtained at four angles where molecules are parallel or perpendicular to the incidence plane. If the director has a certain angle from the surface (pretilt angle), the director is never perpendicular to the incidence plane, so that two minima with zero reflectance and two minima with finite reflectance would result. With increasing pretilt angle, two minima increase and eventually disappear leaving two peaks.

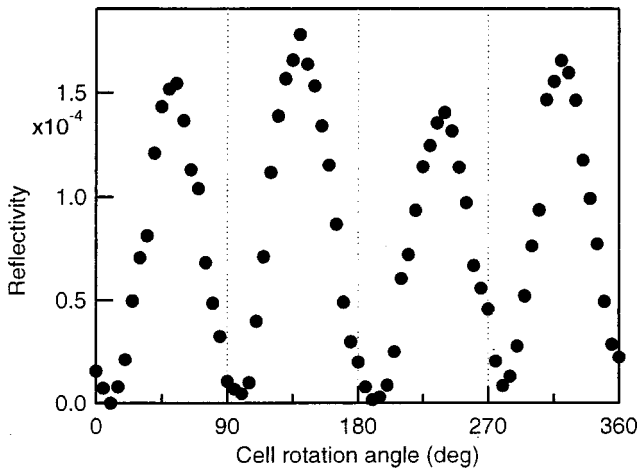

FIG. 3. Reflectivity as a function of cell rotation angle for the incidence angle of 68° in the Sm-*A* phase (65 °C). Four minima with zero reflectance are observed, indicating that the director is parallel to the surface.

If the director is not uniformly oriented but twists in the region near the surface, the pattern changes to that shown in Fig. 2(b). In this figure the transmittance is calculated under the assumption of a twist of 20° in a 50-nm region at a surface. In this case, four minima of zero reflectance appear and every second peak gives a different maximum in reflectivity. These simulated results are for a simple molecular orientation, where the director is always parallel to the surface and twist is confined to be near the surface. The situation is much more complicated in the Sm-C^* phase, since the azimuthal angle distribution on a smectic cone has to be considered.

The purpose of this paper is to explore qualitative molecular orientation to understand V-shaped switching. Hence we will not show further simulated results. For quantitative comparison of the experimental results with the simulation, more realistic molecular orientation including azimuthal angle distribution and layer tilt is necessary to be considered.

IV. RESULTS AND DISCUSSION

A. Sm-*A*

First of all, texture observation was made in the Sm-*A* phase (65 °C). It was found that the layer normal in the bulk is oriented between the two rubbing directions, i.e., 10° from each of them. We define this angle β_L as the angle between the layer normal and the rubbing direction at the top surface and as being positive for clockwise rotation from the rubbing direction (see right bottom in Fig. 1). Here $\beta_L = -10°$ for the bulk.

ATIR measurements were made only under static conditions. One example of the signal profiles is shown in Fig. 3, where the incidence angle of 68° was used and the cell rotation angle α is zero when the rubbing direction is in the optic plane. There are four angles showing minima, which correspond to the angles where LC molecules are parallel or perpendicular to the incidence plane, as shown in the simulated results. The comparison of the experiment (Fig. 3) with the

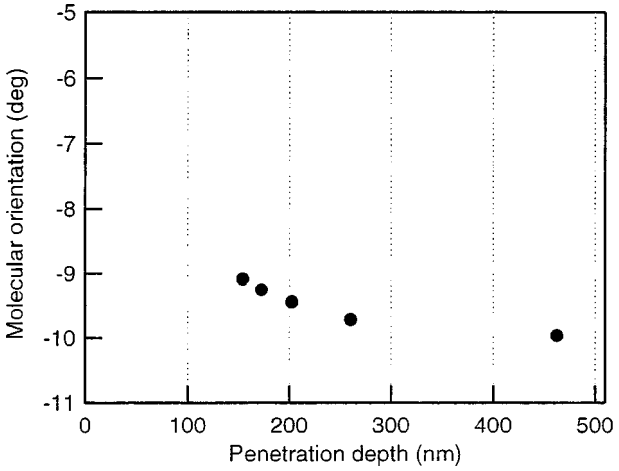

FIG. 4. The director orientation angle in the Sm-A^* phase with respect to the rubbing direction β_M as a function of penetration depth.

simulated results [Fig. 2(a)] implies that the LC molecules are parallel to the surface with a pretilt angle of at most 2°. From the location of the minima, we can estimate the director orientation in the vicinity of the surface. Figure 4 shows the director orientation angle with respect to the rubbing direction as a function of penetration depth. This figure shows that the director tends to rotate toward the rubbing direction when approaching the surface, though the director orientation farther than 450 nm from the surface is almost the same as that in the bulk ($\beta_M = -10°$). Here the angle β_M is positive for clockwise rotation from the rubbing direction, same as β_L. Without the quantitative penetration depth dependence of the director orientation shown in Fig. 4, we can readily notice the molecular twist from a comparison between the shape of the simulated result [Fig. 2(b)] and the experimental one (Fig. 3); namely every second peak shows different reflectivity in the twisted geometry.

B. Sm-X^*

A few zigzag defects in the Sm-X^* phase showing V-shaped switching are found in texture observation, indicating the existence of a chevron layer structure [20]. The optical measurements were made in the region where the chevron tip points antiparallel to the rubbing direction. By applying an electric field in the Sm-X^* phase (50 °C), the maximum rotation of the extinction direction was obtained at ± 7.3 V and the apparent tilt angle was $\pm 33.0°$. It was confirmed that the electrooptic response in the bulk gives an ideal V-shaped switching between 0.1 and 50 Hz, the same as that reported previously [8].

Now we turn to the dynamic ATIR results in the Sm-X^* phase (50 °C). Figure 5 shows the *s*-polarized-light reflectance in the ferroelectric states (at ± 12 V) as a function of cell rotation angle for the incidence angle of 62°. In both cases, the reflectance has four minima. However, unlike in the Sm-A only two of them give complete extinction. This fact suggests that the molecular long axis is more or less parallel to the surface but with a finite pretilt angle. The comparison with Fig. 2(a) suggests a pretilt angle between 5°

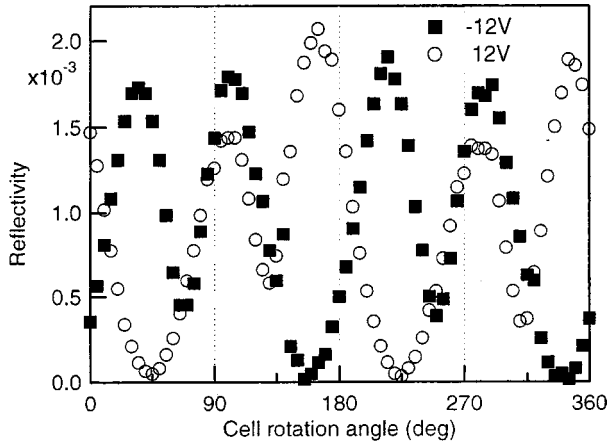

FIG. 5. Reflectivity at the saturation field (under $\pm$ 12 V) in the Sm-X^* phase (50 °C) as a function of cell rotation angle at an incidence angle of 62°. Four minima, two of which give zero reflectance and the others give a small reflectance, are observed, indicating that the director is nearly parallel to the surface.

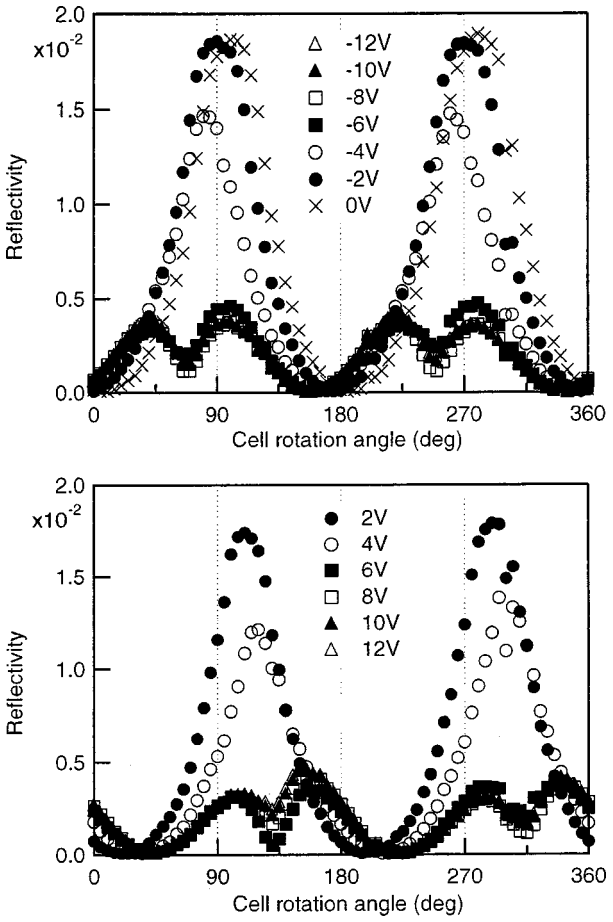

FIG. 6. Reflectivity vs cell rotation angle under various applied voltages during switching on the positive slope for an incidence angle of 60°. Two of the four minima disappear as the voltage decreases to 0 V. This behavior indicates that the director at the surface have a high pretilt angle at 0 V.

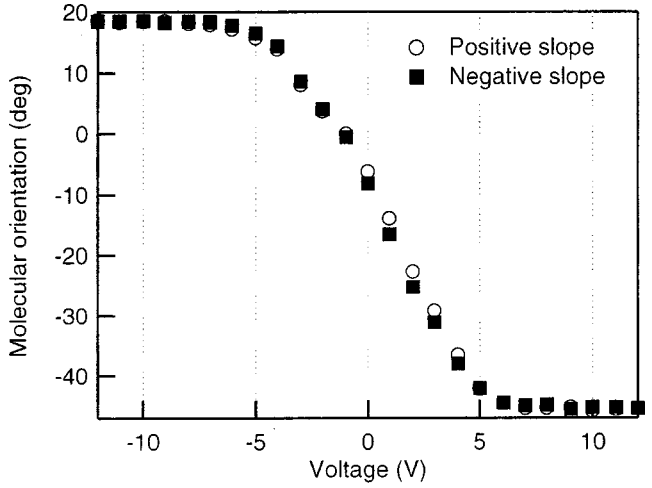

FIG. 7. The angle between the director and rubbing direction β_M as a function of voltage for an incidence angle of 68°.

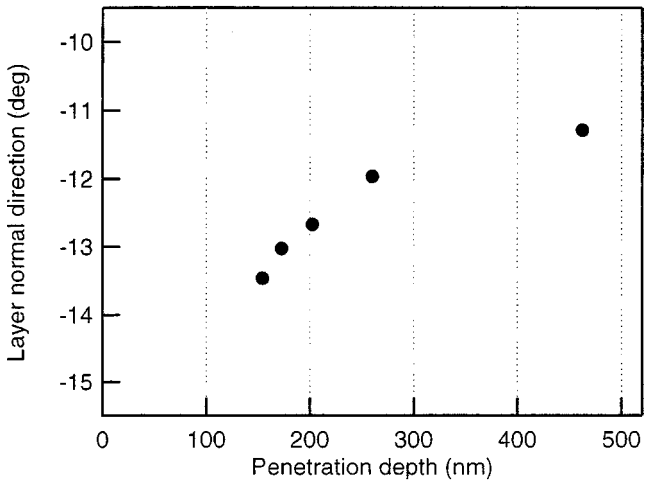

FIG. 8. The layer normal direction β_L determined by the bisector of the two angles in fully switched states as a function of penetration depth. The layer twist is clearly observed near the surface.

and 10°. Shown in Fig. 6 is the reflectance against cell rotation angle during application of a triangular wave field from -12 to $+12$ V for the incidence angle of 60°. This data was taken at various voltages during the switching process. It was found that at lower voltages during switching two of the minima disappeared, and the maximum reflectance increased for all the incidence angles when approaching 0 V. The variation of the profiles is essentially the same as the simulation [Fig. 2(a)] except for their lateral shift. These results suggest that the molecular pretilt angle at the surface becomes a maximum at 0 V, as indicated by several optical measurements in the bulk [8].

Here we want to make a comment on the result in the static condition. A similar measurement to that shown in Fig. 6 was made under short circuit condition ($V=0$). The results for the static (short circuited) and dynamic (0 V) conditions were exactly the same. This means that all the observations obtained under dynamic condition are valid even under static condition.

The minimum reflectance near the rubbing direction ($\alpha=0°$) appears at the angle where the director is in the optic plane. This angle between the director and rubbing direction β_M is plotted as a function of a field in Fig. 7, where the results for the incidence angle of 68° are shown. The results for other incidence angles are essentially the same as those shown in Fig. 7. It is important to note that this behavior is quite similar to the one in the bulk, as reported by Park *et al.* [8]. They have shown that this behavior is qualitatively different from that proposed in the random model and furthermore the changes in optical anisotropy and switching current during V-shaped switching are well simulated using the voltage dependence of apparent tilt angle based on the collective switching of molecules on the tilt cone. Hence we can conclude that molecules near the surfaces switch collectively as in the bulk. The apparent tilt angle at the surfaces is given by half the difference between the angles at the saturation field and is about 31.9°, that is slightly smaller than that in the bulk, 33°. Figure 7 also gives the layer normal direction, that is given by the bisector of the two angles in the fully switched states. The layer normal direction β_L thus determined is displayed in Fig. 8 as a function of penetration depth. Quite interestingly, the layer normal tends to deviate farther from the rubbing direction near the surfaces, i.e., layer twist occurs near the cell surfaces.

Now we examine the director orientation at 0 V near the surfaces. Shown in Fig. 9 is the apparent tilt angle with respect to the layer normal at each penetration depth. The results obtained by dynamic and static measurements agree well with each other. It is clear that the apparent tilt angle becomes larger and the director twists near the cell surfaces. However, the twisting rate with respect to the rubbing direction is not as large, as shown in Fig. 10. This is because the layer normal twists in the opposite sense to that of the director, as already shown in Fig. 8.

In summary, (1) projection of the director onto the surface rotates by 10° from the rubbing direction, (2) the director is in a twisted state at 0 V near the surfaces and the twist angle

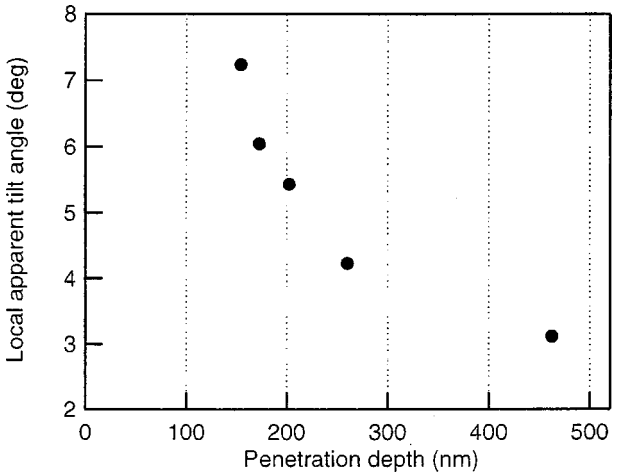

FIG. 9. The apparent tilt angle with respect to the layer normal at each penetration depth at 0 V (dynamic and static). The local apparent tilt angle becomes larger toward the rubbing direction and the molecular long axis forms a twisted orientation near the surface.

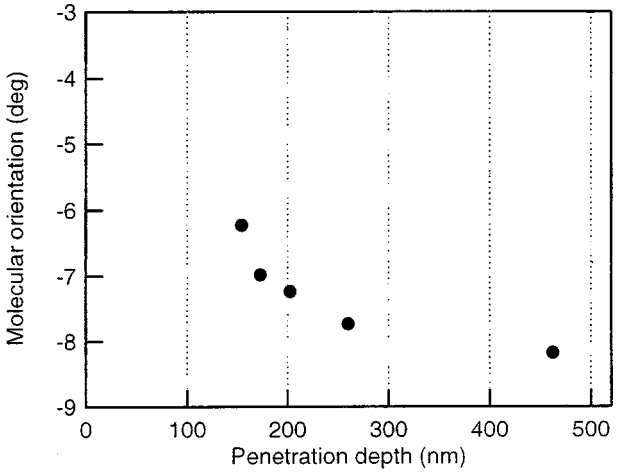

FIG. 10. The direction of the director β_M at 0 V (dynamic and static) with respect to the rubbing direction as a function of penetration depth. Note that the twist angle is reduced due to the compensation by the layer twist shown in Fig. 8.

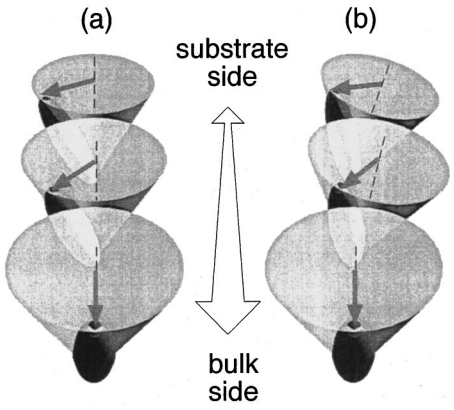

FIG. 11. Schematic illustration of the molecular orientations (a) without and (b) with a layer twist. Arrows and broken lines represent the *c* director and the layer normal. Note that the angles are exaggerated.

at a penetration depth of 150 nm is 7.2° from the optic axis in the bulk. (3) the layer normal also forms a twist configuration near the surfaces, (4) because of the compensation of the twist angles by opposite twist of the director (2) and layer normal (3), the twist angle of the director with respect to the bulk layer normal is relatively small at the same depth, i.e., 3.8°. The situation is illustrated in Fig. 11, in which both cases (a) without and (b) with layer twist are drawn. In the actual case (b), the twist angle with respect to the bulk layer normal is half of that without layer twist. This is the reason why high extinction and a high contrast ratio are obtained during V-shaped switching in the three-component mixture used.

In this way, the layer twist compensates the molecular twist, so that the distortion energy loss caused by the molecular twist is suppressed. This means, however, the layer distortion energy increase by the layer twist must be smaller than the molecular orientational distortion energy decrease by the compensation. It is not easy to prove this condition quantitatively. However, two experimental observations suggest that the layer of this mixture is very soft, so that the layer distortion energy is relatively low. The first evidence for this is given by texture observation. Because of a chevron layer structure, we often notice zigzag defects that easily change their shape. Since the zigzag defect originates from the boundaries of chevron layer structures with different tip directions [21–23], the easy movement of the zigzag defects indicates the softness of the smectic layer. The second evidence was obtained by layer compression measurements [24]. It is known that the layer compression modulus exhibits a softening at the untilted to tilted smectic phase transitions [25]. It generally appears as a sharp decrease and recovery of the modulus at the transition, showing a cusplike structure. In the present mixture, on the other hand, the softening occurs like typical untilted-tilted phase transitions, but the small modulus below the Sm-*A*-Sm-*X** phase transition does not recover back to the value in the Sm-*A* phase and sharply increases at the transition from Sm-*X** to a low-temperature antiferroelectric phase. This experiment also indicates that the layers of the present mixture are soft, though the physical property obtained by this experiment is a layer compression modulus but not an elastic modulus for layer twist.

V. CONCLUSIONS

ATIR measurements were performed to investigate the molecular orientation and switching near surfaces. It was found that layer twist occurs near the surfaces and it is compensated by twisting of the director with the opposite sense, resulting in a relatively small orientation change of the molecular long axis in the cells. We conclude that this is the reason why V-shaped switching in the three-component mixture shows high extinction and has a high contrast ratio. To conclude that the soft layer is a necessary condition for V-shaped switching, the measurements using other compounds showing V-shaped switching are needed. The present experiment supports the role played by polarization charge effect, but also implies that the phenomenon of V-shaped switching is not so simple. For further analysis, the quantitative comparison of the experimental results with the theoretical prediction is expected. This effort is under way in our laboratory by calculating the reflected light by applying the 4×4 matrix method to the evanescent region. The results will be reported in the near future.

ACKNOWLEDGMENTS

This work is partly supported by Grant-in-Aid for Scientific Research on Priority Area (A) (11167232) and on Priority Area (B) (12129202), by the Ministry of Education, Science, Sports and Culture, the JSPS Research for Future Program (JSPS-RFTF98R14201), and NEDO international collaboration Fund (98MB1). We are grateful to Dr. D. R. Link for a critical reading of this manuscript.

[1] S. Inui, N. Iimura, T. Suzuki, H. Iwane, K. Miyachi, Y. Takanishi, and A. Fukuda, J. Mater. Chem. **6**, 71 (1996).
[2] A. Fukuda, *Proceedings of the 15th International Display Research Conference, Asia Display '95, Hamamatsu, 1995* (unpublished).
[3] A. Fukuda, S. S. Seomun, T. Takahashi, Y. Takanishi, and K. Ishikawa, Mol. Cryst. Liq. Cryst. **303**, 379 (1997).
[4] K. Nito, T. Fujioka, N. Kataoka, and A. Yasuda, *Digest of Technical Papers, AM-LCD 94, 1994* (unpublished).
[5] Y. Asao, T. Togano, M. Terada, T. Moriyama, S. Nakamura, and J. Iba, Jpn. J. Appl. Phys. **38**, 5977 (1999).
[6] J. Fünfschilling and M. Schadt, J. Appl. Phys. **66**, 3877 (1989).
[7] T. Matsumoto, A. Fukuda, M. Johno, Y. Motoyama, T. Yui, S.-S. Seomun, and M. Yamashita, J. Mater. Chem. **9**, 2051 (1999).
[8] B. Park, S. S. Seomun, M. Nakata, M. Takahashi, Y. Takanishi, K. Ishikawa, and H. Takezoe, Jpn. J. Appl. Phys. **38**, 1474 (1998).
[9] B. Park, M. Nakata, S. S. Seomun, Y. Takanishi, K. Ishikawa, and H. Takezoe, Phys. Rev. E **59**, R3815 (1998).
[10] P. Redquist, J. P. F. Lagerwall, M. Buivydas, F. Gouda, S. T. Lagerwall, N. A. Clark, J. E. Maclennan, R. Shao, D. A. Coleman, S. Bardon, T. Bellini, D. R. Link, G. Natale, M. A. Glaser, D. M. Walba, M. D. Wand, and X.-H. Chen, J. Mater. Chem. **9**, 1257 (1999).
[11] B. Park, M. Nakata, T. Ogasawara, Y. Takanishi, K. Ishikawa, and H. Takezoe, *SID 99 Digest of Technical Papers, San Jose, 1999*, edited by J. Morreale (unpublished).
[12] B. Park, M. Nakata, T. Ogasawara, Y. Takanishi, K. Ishikawa, and H. Takezoe, *Digest of Technical Papers, AM-LCD 99, Tokyo, 1999* (unpublished).
[13] N. A. Clark, D. Coleman, and J. E. Maclennan, Liq. Cryst. **27**, 985 (2000).
[14] M. Nakata, S. Ikeda, T. Ogasawara, Y. Takanishi, K. Ishikawa, and H. Takezoe, Proc. SPIE **3955**, 45 (2000).
[15] S. S. Seomun, T. Gouda, Y. Takanishi, K. Ishikawa, H. Takezoe, and A. Fukuda, Liq. Cryst. **26**, 151 (1999).
[16] A. D. L. Chandani, Y. Cui, S. S. Seomun, Y. Takanishi, K. Ishikawa, H. Takezoe, and A. Fukuda, Liq. Cryst. **26**, 167 (1999).
[17] S. Tanaka and M. Yamashita, Jpn. J. Appl. Phys. **38**, L139 (1999).
[18] N. J. Mottram and S. J. Elston, Liq. Cryst. **26**, 1853 (1999).
[19] S.-L. Wu and W.-J. Hsieh, Chem. Mater. **11**, 852 (1999).
[20] Y. Takanishi, T. Ogasawara, K. Ishikawa, H. Takezoe, Y. Takahashi, and A. Iida, Jpn. J. Appl. Phys. **40**, 728 (2001).
[21] Y. Ouchi, H. Takano, H. Takezoe, and A. Fukuda, Jpn. J. Appl. Phys. **27**, 1 (1988).
[22] N. Hiji, Y. Ouchi, H. Takezoe, and A. Fukuda, Jpn. J. Appl. Phys. **27**, L1 (1988).
[23] N. A. Clark and T. P. Rieker, Phys. Rev. A **37**, 1053 (1988).
[24] S. Shibahara, J. Yamamoto, Y. Takanishi, K. Ishikawa, and H. Takezoe, Phys. Rev. **5**, 1707 (2001).
[25] S. Shibahara, J. Yamamoto, Y. Takanishi, K. Ishikawa, H. Takezoe, and H. Tanaka, Phys. Rev. Lett. **85**, 1670 (2000).